

NUCLEATION AND δ TO γ PHASE TRANSFORMATION AT THE SURFACE OF RAPIDLY SOLIDIFIED LOW CARBON STEELS

L.Strezov⁽¹⁾, T.Evans⁽¹⁾, K.Mukunthan⁽¹⁾, J.Herbertson⁽²⁾

(1) BHP Minerals Technology, Australia, (2) Sky Point Innovations, Australia.

ABSTRACT

Nucleation and δ to γ phase transformation on the surface of low carbon steels, under the conditions approximating the meniscus region of a twin roll caster, were studied using an arrangement of two-colour optical fibre pyrometry. The largest nucleation undercooling, measured with the 0.5 mm diameter optical fibre, was around 180K, corresponding to the spatial average undercooling over the “observed” area of the solidifying surface. For the same experimental conditions, the 0.1 mm diameter optical fibre gave nucleation undercoolings of up to 1000K, corresponding to the model estimate of actual undercooling at the points of direct melt/substrate contact. Transient nucleation modelling showed that formation of δ phase was not possible under these conditions and a metastable quasi-crystalline phase would form for a brief period of several milliseconds, subsequently transforming into a crystalline phase. The very large undercoolings were associated with surface solidification structures comprised of concentric rings around the nucleation sites. Compositional analysis across the rings revealed no traces of microsegregation suggesting diffusionless growth associated with high growth rates. The δ to γ phase transformation was followed by monitoring the changes in the emittance of the solidifying surface. The phase transformation temperatures, such as liquid to δ and δ to γ could be easily determined for the low cooling rate conditions. For the high cooling rate conditions, the nucleation temperature appeared to be much lower by about 100K and the δ phase seemed to be absent. The results presented here suggest that the very high cooling rates experienced during nucleation at the points of contact, can lead to suppression of the δ phase and nucleation of a metastable glass phase, followed by re-crystallisation and solidification into γ phase at the surface of a solidifying low carbon strip.

INTRODUCTION

It has generally been accepted that most industrial metal casting processes proceed with heterogeneous nucleation. The reason for this assumption is the fact that the presence of mould surface, solid phases and impurities can potentially act as nucleants, thus reducing the free energy barrier for nucleation. In the area of near net shape casting, such as twin roll casting of steel strip, understanding of the processes taking place at the strip surface, such as nucleation, growth and solid state transformations are of paramount importance. The wetting of the substrate by the melt, has been shown to have a dominating influence on the interfacial heat transfer and consequently on the microstructural development (1). Improved wetting will reduce the energy barrier for nucleation while at the same time increasing the cooling rate of the liquid. Since the overall nucleation rate is controlled both by the rate of cluster formation and the rate of atom transfer to the nucleus, a critical cooling rate will exist above which the nucleation rate is expected to reduce. The purpose of this work is to establish the relevant nucleation mechanism under the conditions prevailing at the meniscus region of a twin roll caster, and examine the implications to the subsequent growth and δ to γ transformation at the surface of a solidifying low carbon steel strip.

EXPERIMENTAL DETAILS

Experiments were conducted using an immersion apparatus that allowed for controlled experimental conditions such as substrate velocity and residence time in the melt, gas atmosphere and melt superheat. It has been shown that this experimental apparatus simulates the conditions of interfacial heat transfer and solidification structures of a twin roll caster(1). The details of the equipment and its workings have been described elsewhere(2). A schematic diagram of the immersion apparatus is presented in Fig 1.

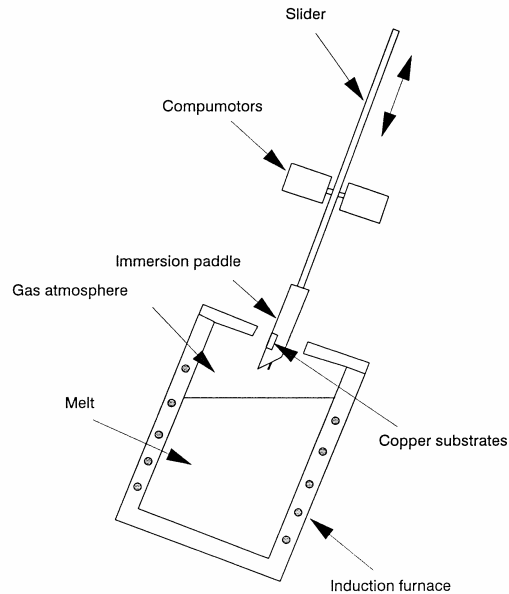


Fig.1 Immersion apparatus

Shell surface temperature measurement was achieved by boring a 0.5 mm diameter hole through the substrate, at the end of which an optical fibre of the same diameter was positioned. The optical fibre guided light from the exposed melt surface to a two colour pyrometer. The pyrometer was optimised such that it had a response time of less than one microsecond. Further details of the pyrometer and its operation are provided by Evans (3). The intensity of the light at two wavelengths (0.99 μm and 1.01 μm) was acquired at a frequency of 12 kHz. The ratio of the two signals was proportional to the actual strip surface temperature. For all immersion experiments, the melt temperature was maintained at approximately 1570 °C and the initial substrate temperature at about 25 °C. The substrate arrangement for shell surface temperature measurement is depicted in Fig 2.

The substrate surface was a ridged texture comprising of ridges parallel to the immersion direction at a spacing of 180 μm and depth of 20 μm . The substrate was made from copper and the surface was chrome plated. The immersion velocity of the substrate into the metal bath of low carbon steel was set at 1m/s for all experiments, which gave a mean substrate residence time below the melt surface of 0.19s.

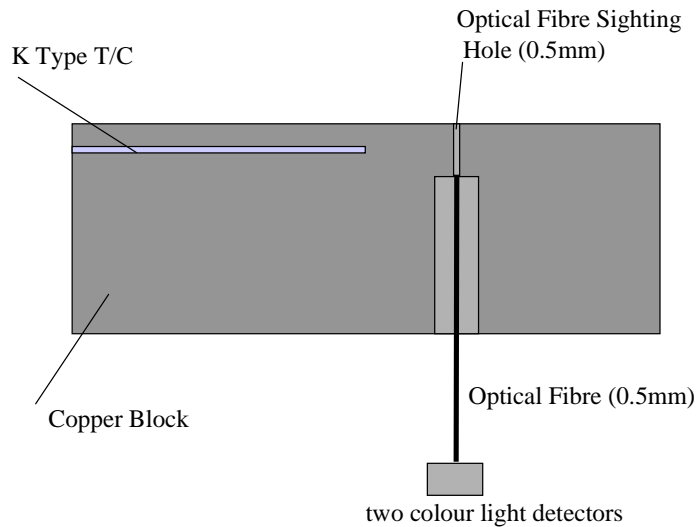


Fig. 2 Substrate assembly showing the optical fibre arrangement

It has been shown previously that after each immersion of a substrate in a steel bath, the substrate surface was coated with a thin layer of MnO-SiO₂ powder (4). When this oxide layer was allowed to build-up and melt, the interfacial heat transfer increased dramatically and the surface solidification structures changed in morphology. For the purpose of the present work, the substrate “oxide layer” was allowed to build-up and melt. The immersion sequence started with a “clean” substrate surface and was completed when there was visual evidence that the accumulated oxide had melted.

RESULTS AND DISCUSSION

Fig. 3 shows the measured strip surface temperatures during the first 50ms of melt/substrate contact, for the conditions of “clean” substrate surface and when the “oxide” layer was allowed to build up. In both cases, the strip surface temperature reduced rapidly after contact, from the initial melt temperature to a minimum, after which recalescence was observed. This minimum temperature was identified as the nucleation temperature and was significantly lower for the “oxide build-up” case, with a nucleation undercooling of 152 K. The average nucleation cooling rate was calculated by dividing the difference between the initial melt temperature and temperature by the time to nucleation. Fig. 4 presents the relationship between the cooling rate and nucleation temperature for a variety of experimental conditions. Increasing the cooling rate made nucleation more difficult with an overall effect of reducing the nucleation temperature.

It is reasonable to expect that the introduction of a 0.5 mm hole in the substrate to provide shell temperature measurement would affect the actual shell temperature. The optical fibre collected light from the total melt surface exposed through the hole in the substrate, thus actually measuring the spatial average temperature over that area. The nucleation events could be assumed to take place at the points of intimate melt/substrate contact, at the sharp corners, around the perimeter of the hole. Hence, it is expected that the cooling rate at the true area of contact between the substrate and the melt is significantly higher than the experimental measurement. By the same analysis the nucleation temperature would be much lower than the one measured.

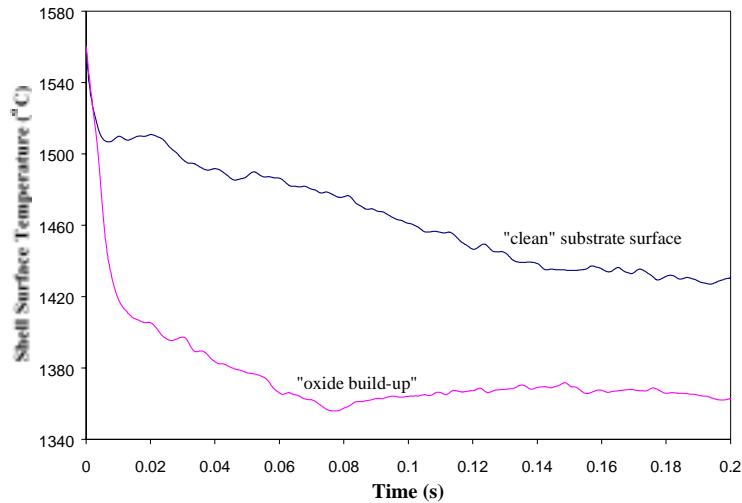


Fig. 3 Strip surface temperature

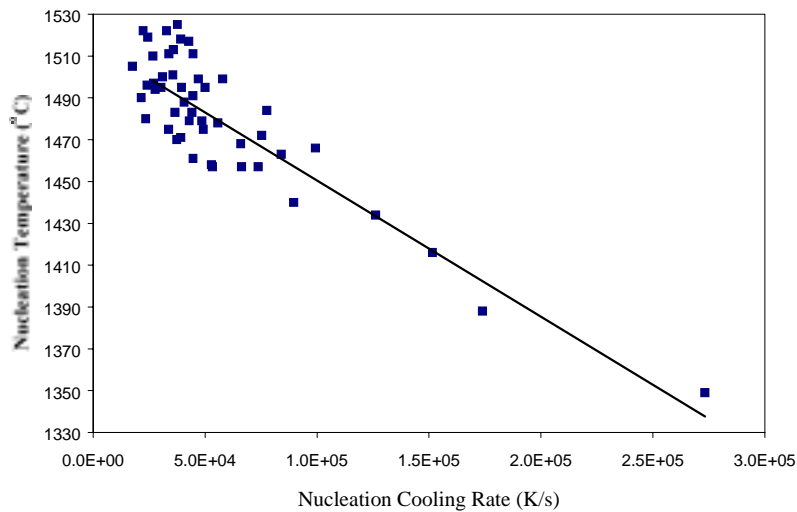


Fig. 4 Nucleation temperature and cooling rate

Thermal modelling of the microscopic environment in the region around the hole showed that the local cooling rate was approximately one order of magnitude larger, at the corners around the perimeter of the hole, than the measured spatial average (5,6). The predicted cooling rate due to the averaging effects of the optical fibre measurements, as well as the actual nucleation cooling rate together with experimental data have been plotted against the time to nucleation in Fig. 5. The predicted spatial average cooling rate correlated well with all of the experimental data from this work, indicated by open points, and experimental work by Todoroki et al(7), given by closed diamonds, as well as experimental work by Mizukami et al. (8), indicated by closed squares. The same modelling work also predicted that a massive nucleation undercooling of around 1000 K was possible.

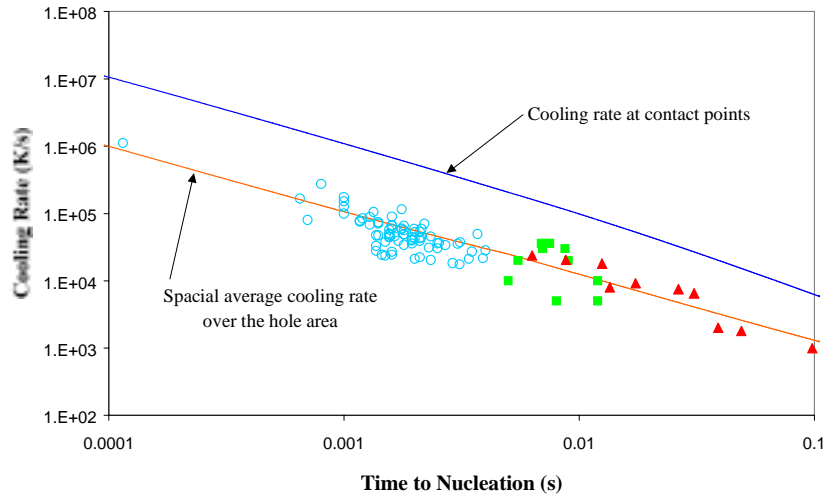


Fig. 5 Model prediction of nucleation cooling rate

To test the model predictions, a second smaller hole and fiber of 0.1 mm diameter was employed in the same substrate adjacent to the 0.5 mm hole. This allowed for a direct comparison of the effect of the size of the hole, i.e. spatial temperature averaging, on the measured data. The surface temperatures for both measurements are presented in Fig. 6. For the same experiment, the 0.1 and 0.5 mm holes gave nucleation temperatures of 498 and 1373°C, respectively. The nucleation undercooling was 1027K for the 0.1 mm and 152K for the 0.5 mm hole, corresponding well to the model prediction.

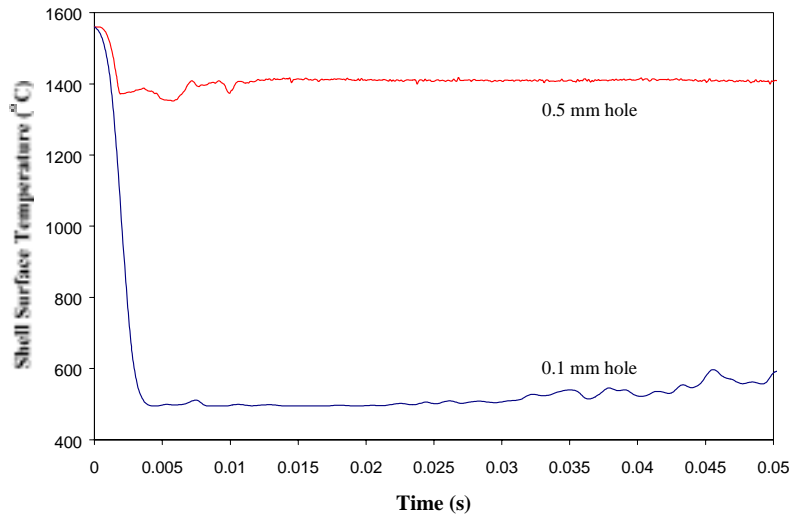


Fig. 6 Strip surface temperature for 0.1 and 0.5 mm hole

The massive undercoolings at the points of melt/substrate contact raise the question as to which phase is likely to nucleate first under these conditions. This aspect was further investigated by employing a transient nucleation model which details have been published previously (6,9). The time-temperature-transformation diagram as predicted by this nucleation modelling is presented in Fig. 7. This figure shows the calculated δ phase fields for a melt/substrate wetting angles of 45° , 90° and 180° . It has been shown that the contact angle for this system is around 110° (3). Also presented in this figure are the *Spatially averaged nucleation temperature*, calculated as the spatial average of the melt interface over

the area of the hole, and the *Actual nucleation temperature* at the contact points, as calculated from the heat transfer model.

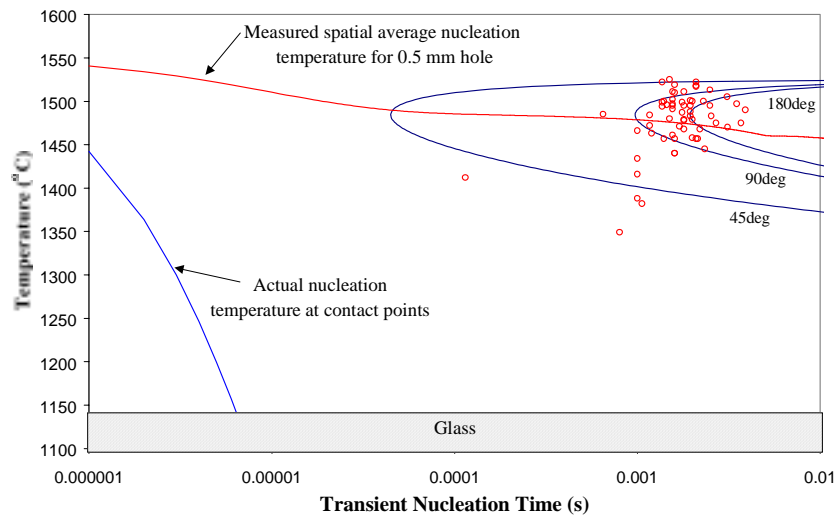


Fig. 7 Transient nucleation for low carbon steel system

The information contained in this figure suggests that it is possible to achieve massive undercoolings at the points of nucleation, as well as completely miss the δ region and form a glass phase. Some supportive evidence for the very high cooling rates was found at the strip surface. Fig. 8 shows the as cast strip surfaces for low and high cooling rate conditions. The sample produced at low cooling rates (Fig. 8a) exhibited surface dendrites around the nucleation points. The sample produced at high cooling rates (Fig. 8b) showed absence of dendritic growth. A banded structure was visible around the nucleation points. X-ray mapping of this region failed to detect any microsegregation suggesting diffusionless solidification, likely to be taking place at high cooling rates. Since the structure in this region was crystalline at room temperature, one can conclude that this phase was metastable and must have re-crystallised at some stage during the solidification. On re-crystallisation, the release of latent heat would reheat the shell. If the partially solidified shell was reheated into the δ -phase field, the final solidification structure would not be substantially different from the normal low-carbon steel as cast structure. However, should re-heating occur only into the γ -phase field, an austenitic solidification structure is expected. Obviously, a combination of both is also possible.

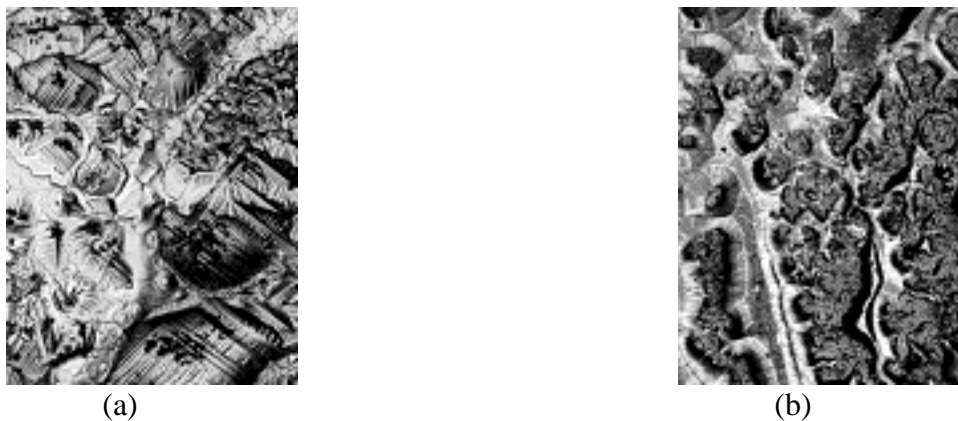


Fig. 8 Surface solidification structures for low (a) and high nucleation cooling rates

In order to study the transformation phenomena taking place at the surface of the solidifying strip a new technique was developed based on the pyrometry temperature measurement. This technique relied on monitoring the changes in the emittance of the surface of the solidifying strip at a given temperature relative to the emittance of the liquid metal. The technique was first trailed on electrolytic iron, slowly cooled from liquid to room temperature. The “relative emittance” of the surface of the solidifying electrolytic iron sample exhibited significantly different temperature dependence for the liquid, δ and γ phases, allowing for the phase transformation temperatures to be accurately determined (Fig. 9).

The same analysis was then applied to the already measured data from the immersion experiments. Fig. 10 presents the “relative emittance” as a function of temperature for low and high cooling rate conditions. The phase transformation temperatures, such as liquid to δ and δ to γ could be easily determined for the low cooling rate conditions (Fig. 10a). For the high cooling rate conditions, the nucleation temperature appeared to be lower by about 100K and the δ phase seemed to be absent (Fig. 10b). It appears that the solidification of the surface of the low carbon strip took place in the austenite phase where the liquid to γ transformation temperature was well below the stable δ phase region (1427°C).

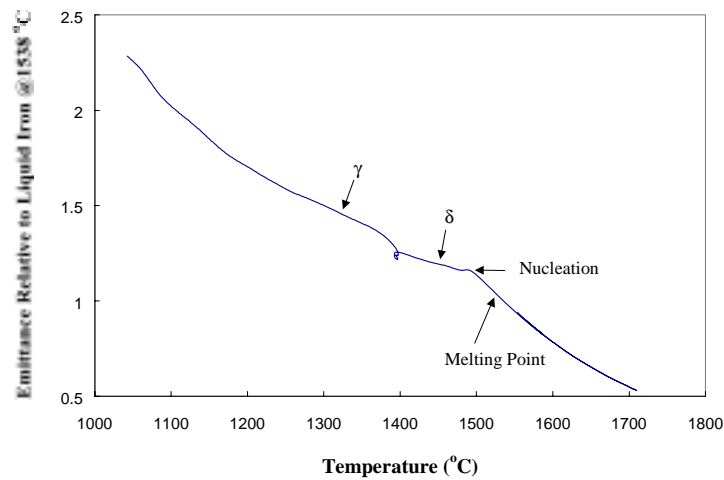
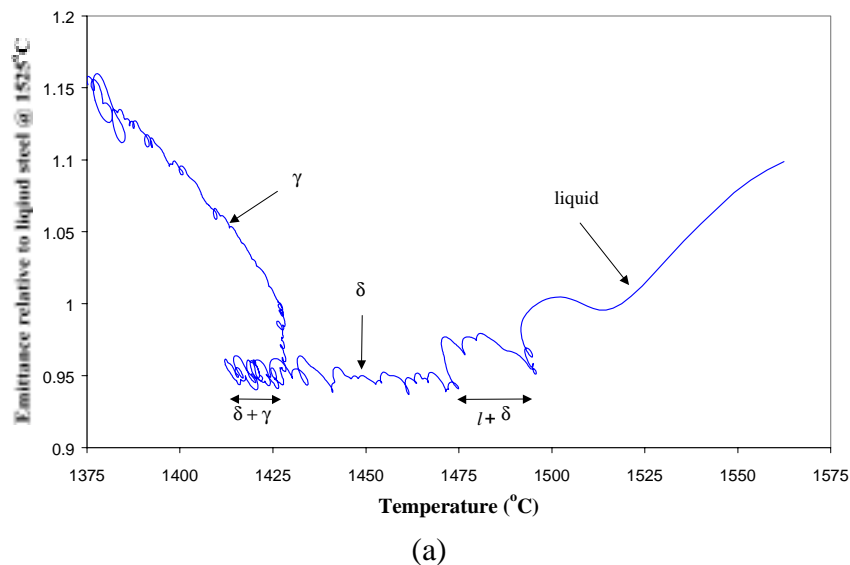


Fig. 9 Emittance of iron relative to liquid iron at 1538°C



(a)

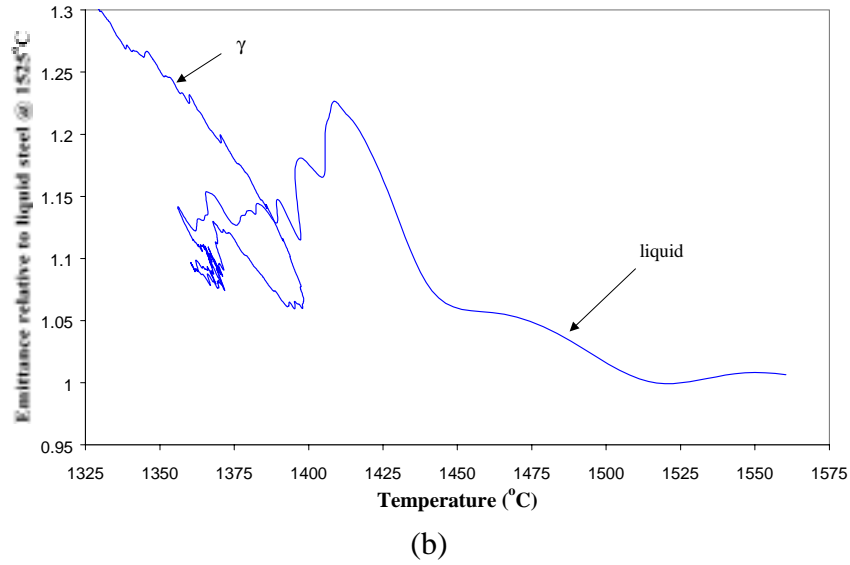


Fig. 10 Relative emittance as a function of temperature for low (a) and high (b) cooling rate conditions

Notwithstanding the limitations of these techniques and the inherent averaging across the area of the hole, the results presented here suggest that the very high cooling rates experienced during nucleation at the points of contact, can lead to suppression of the δ phase and nucleation of a metastable glass phase, followed by re-crystallisation and solidification into γ phase at the surface of a solidifying low carbon strip.